Pergamon

PII: S0149-7634(97)00014-6

Generation of Theta and Gamma Rhythms in the Hippocampus

L. STAN LEUNG*

Department of Physiology and Clinical Neurological Sciences, University Campus, London Health Sciences Centre, University of Western Ontario, London, Ontario N6A 5A5, Canada

LEUNG, L. S. *Generation of theta and gamma rhythms in the hippocampus.* NEUROSCI BIOBEHAV REV **22**(2), 275–290, 1998.—In the behaving rat, theta rhythm was dominant during walking and rapid-eye-movement sleep, while irregular slow activity predominated during immobility and slow-wave sleep. Oscillatory evoked potentials of 20–50 Hz and spontaneous fast (gamma) waves were more prominent during theta compared with non-theta behaviors. The oscillations were simulated by a systems model with recurrent inhibition. The model also predicts a behaviorally dependent inhibition, which was confirmed experimentally using paired-pulse responses. Paired-pulse facilitation (PPF) of the population spikes in CA1 was larger during walking than immobility, mostly mediated by a cholinergic input. Spike responses in vitro were characterized by a relative lack of inhibition or disinhibition compared with the behaving rat. The two-input, two-dipole model of the theta rhythm in CA1 is reviewed. Afferents to the CA1 pyramidal cells are assumed to be rhythmic and consist of atropine-sensitive and atropine-resistant inputs driving the somata and distal dendrites, respectively. The atropine-sensitive theta rhythm was mainly caused by a series of Cl^- mediated inhibitory postsynaptic potentials (IPSPs) on pyramidal cells. It is suggested that previous claims of the participation of excitatory postsynaptic potentials (EPSPs) and not IPSPs in the intracellular recordings in vivo were flawed. Single cell recordings in vitro suggested that intrinsic voltage-dependent membrane potential oscillations modulate the response to a theta-frequency driving. Membrane potentials of pyramidal cells in vitro showed resonance in the theta frequency range. © 1998 Elsevier Science Ltd. All rights reserved.

Paired-pulse facilitation   Population spikes   Cholinergic   Membrane potential oscillations   Behavior   Sleep

HIPPOCAMPAL EEG VARIES WITH BEHAVIOR

VANDERWOLF (94) was the first to emphasize the correlation of the hippocampal EEG with the moment-to-moment behavior of the rat (Fig. 1). He stated that

''Trains of rhythmical 6–12 c/sec waves in the hippocampus and medial thalamus precede and accompany gross voluntary types of movement such as walking, rearing, jumping, etc. Behavioral immobility (in the alert state) and automatic movement patterns such as blinking, scratching, washing the face, licking or biting the fur, chewing food or lapping water are associated with irregular hippocampal activity'' (94)

In addition, 6–12 Hz waves in the hippocampus or the hippocampal theta rhythm were found during rapid-eye-movement sleep but not during slow-wave sleep (Fig. 1). Subsequently, Vanderwolf showed that theta rhythm in the walking rat is resistant to atropine ((46,95); Fig. 2) and mediated by serotonin (96,97). In contrast, the low-frequency theta rhythm elicited by reticular stimulation (46) or preceding an avoidance response (95) and the theta rhythm in anesthetized animals was sensitive to atropine ((46,92,96); Fig. 2). These findings of Vanderwolf

emphasize a dynamic modulation of the spontaneous hippocampal EEG in the behaving rat by different types of modulating inputs.

Theta or irregular activity may define a functional state of the hippocampus (cf. ref. (22)). My research on the electrophysiology of the hippocampus began as an attempt to define the 'theta state', a brain state accompanied by a theta rhythm. The work was inspired by the work of Case Vanderwolf, who showed a clear correlation of the hippocampal theta rhythm and its pharmacology with the behavior of the animal. Part of my Ph.D. thesis (in Walter Freeman's laboratory at Berkeley) dealt with the characterization of neural systems, which I applied to the hippocampus in the behaving rat. In this review, I shall first summarize results on evoked (impulse) responses in the hippocampus during theta and non-theta brain states. The evoked and spontaneous rhythms of the hippocampus share a frequency of about 40 Hz, also known as the gamma rhythm (16,31,87). Then, I shall review the spatial and rhythmic generation of the theta rhythm. I shall not speculate on the functional importance of the hippocampal rhythms, though their mechanisms of generation reviewed here are germane to this issue.

---

* Tel.: (519) 663 3733; Fax: (519) 661 3827; E-mail: sleung@julian.uwo.ca.

AWAKE

hippo-
campus

walking   immobile

neocortex

ASLEEP

hippo-
campus

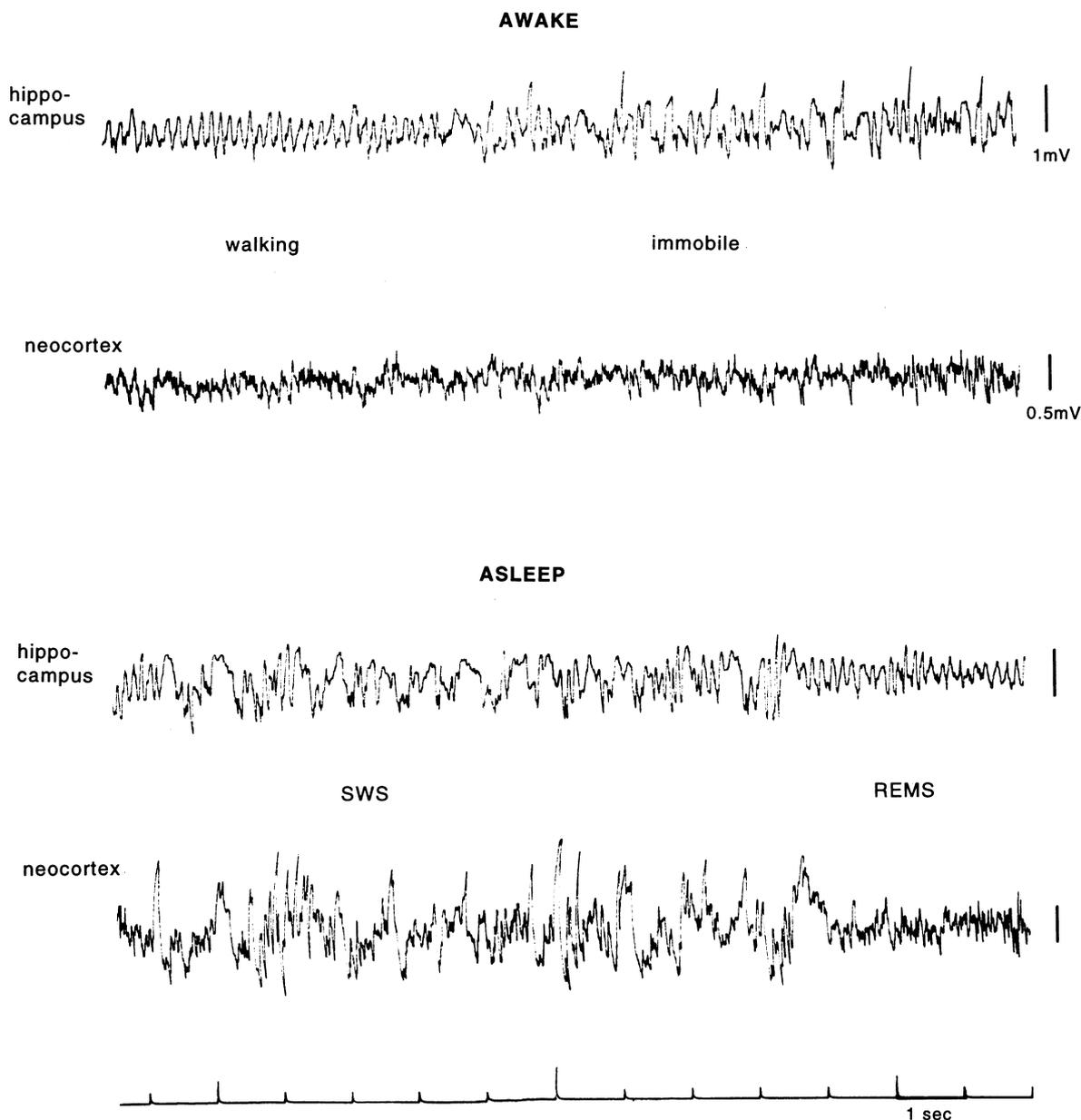SWS   REMS

neocortex

1 sec

FIG. 1. Dependence of hippocampal EEG on the moment-to-moment behavior of the rat during the waking (top) and sleep states (bottom). Top: clear theta rhythm of about 7 Hz accompanied walking in the rat, while large irregular slow activity dominated during immobility. The neocortical EEG was desynchronized when the rat was awake. Bottom: there was slower irregular slow activity (delta waves larger) in the hippocampus and neocortex during slow wave sleep (SWS). The neocortical EEG desynchronized and the hippocampal EEG changed to a theta rhythm when the rat entered rapid-eye-movement sleep (REMS).

EVOKED AND SPONTANEOUS OSCILLATIONS (20–50 Hz) IN THE HIPPOCAMPUS

When the Schaffer collaterals were stimulated by an electrical shock, a negative wave was observed in the apical dendrites of the CA1 pyramidal cells (Fig. 3); this negative wave reversed to a positive wave at the CA1 cell body layer. The apical dendritic negative wave was the population excitatory postsynaptic potential (EPSP). Increasing the stimulus intensity would induce a population spike, a synchronous firing of action potentials (3,60), best seen at or near the cell body layer. Schaffer collateral evoked responses showed a robust correlation with behavior. The initial slope and peak of the EPSP was smaller during walking than

immobility, and the average evoked responses at low intensity showed oscillations of about 20–50 Hz ((51); Fig. 3). At an intensity that evoked a population spike, the spike was smaller during walking than immobility (51). The dependence of the CA1-evoked response on behavior, including the oscillatory response during walking, was mostly abolished by atropine sulfate (Fig. 3).

Recurrent inhibition has been suggested as the main cause of the oscillatory response in CA1 (51,52,58). A Schaffer collateral shock excites pyramidal cells (PYR), which in turn excite inhibitory interneurons (INT) that provide feedback inhibition on PYR (Fig. 4). PYR are assumed to have sufficient tonic activity such that PYR inhibition results in a suppression of excitation to the INT and the disinhibition of
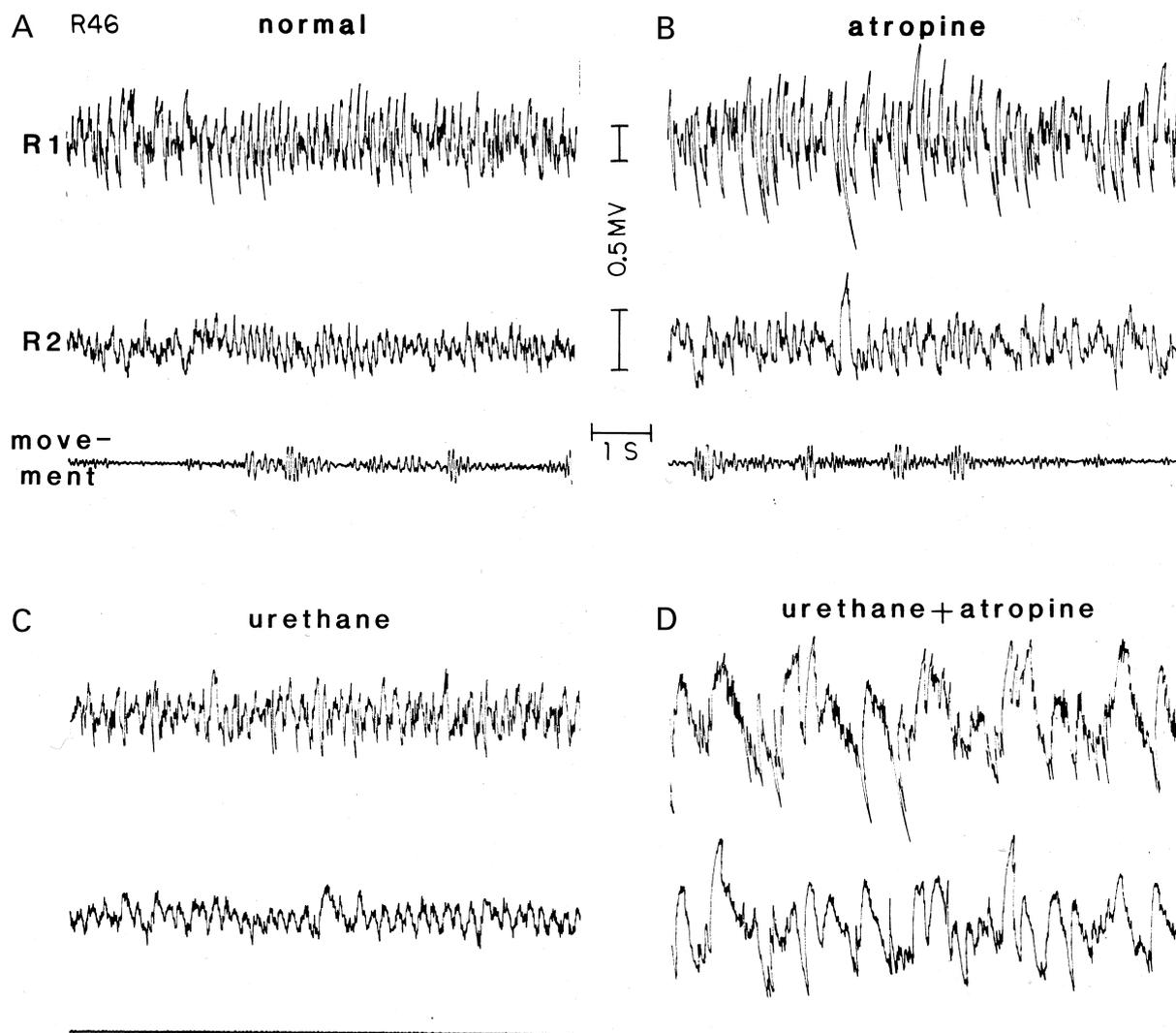
FIG. 2. Hippocampal theta was atropine-resistant in the behaving rat and atropine-sensitive under urethane anesthesia. (A) Hippocampal EEG recorded at the apical dendrites (R1) or alveus of CA1 (R2), concomitant with a magnet and coil movement sensor signal. Hippocampal EEG showed theta during movement. (B) Atropine sulfate (25 mg kg^{-1} i.p.) did not abolish hippocampal theta. (C) Under urethane anesthesia (1 g kg^{-1} i.p.), tail pinch generated a slow rhythm (5–6 Hz theta). (D) The slow rhythm in (C) was abolished by atropine sulfate (25 mg kg^{-1} i.p.).

PYR. A cycle of activity is as follows: PYR excitation, INT excitation, PYR inhibition, INT disexcitation, PYR disinhibition (equivalent to excitation), and the cycle may repeat again. The recurrent inhibition model has one major non-linearity which effectively impedes oscillations in the immobile rat. During walking, brainstem inputs are assumed to provide a bias that linearized the circuit, and the responses are oscillatory (52). 'Spontaneous' 20–50 Hz fast (beta and gamma) waves are predicted by the model, assuming that the input is white noise of wide bandwidth (Fig. 5). The spectral distribution of the simulated fast waves resembles that seen in rats during walking (Fig. 5).

The model suggests that fast waves should share the same properties with evoked oscillations, such as a dependence on behavior and cholinergic input. The latter dependence was not apparent in the literature and Stumpf (93), who first studied the fast waves in rabbits in detail, found no such dependence. Using spectral analysis, we showed that hippocampal fast waves in CA1 were more pronounced during walking than immobility ((69); Fig. 5(C)). Subsequently, I showed that fast waves were attenuated by atropine (56) or septal lesion (unpublished data). Fast waves during walking or struggling were slightly increased by eserine in the normal rats (56,71) but they were greatly increased by eserine in the vasopressin-deficient Brattleboro rats (71).

The amplitude of the spontaneous fast waves in CA1 of a normal rat was much smaller than that of the theta rhythm. In a project on hippocampal kindling, I found that CA1 fast waves increased in power by up to ten times for 20–30 min after a hippocampal afterdischarge induced by a Schaffer collateral tetanus (57). The bandwidth of the large postictal fast waves was similar to that of normal fast waves, and they were also attenuated by septal lesion or atropine (57). However, the postictal fast waves showed no clear behavioral correlation with walking and immobility.

The model of recurrent inhibition has been successful in predicting the power spectrum of spontaneous fast EEG oscillations. It appears to be consistent with all existing literature on pyramidal cell and interneuronal interactions.

CONTROL

IMM

WALK
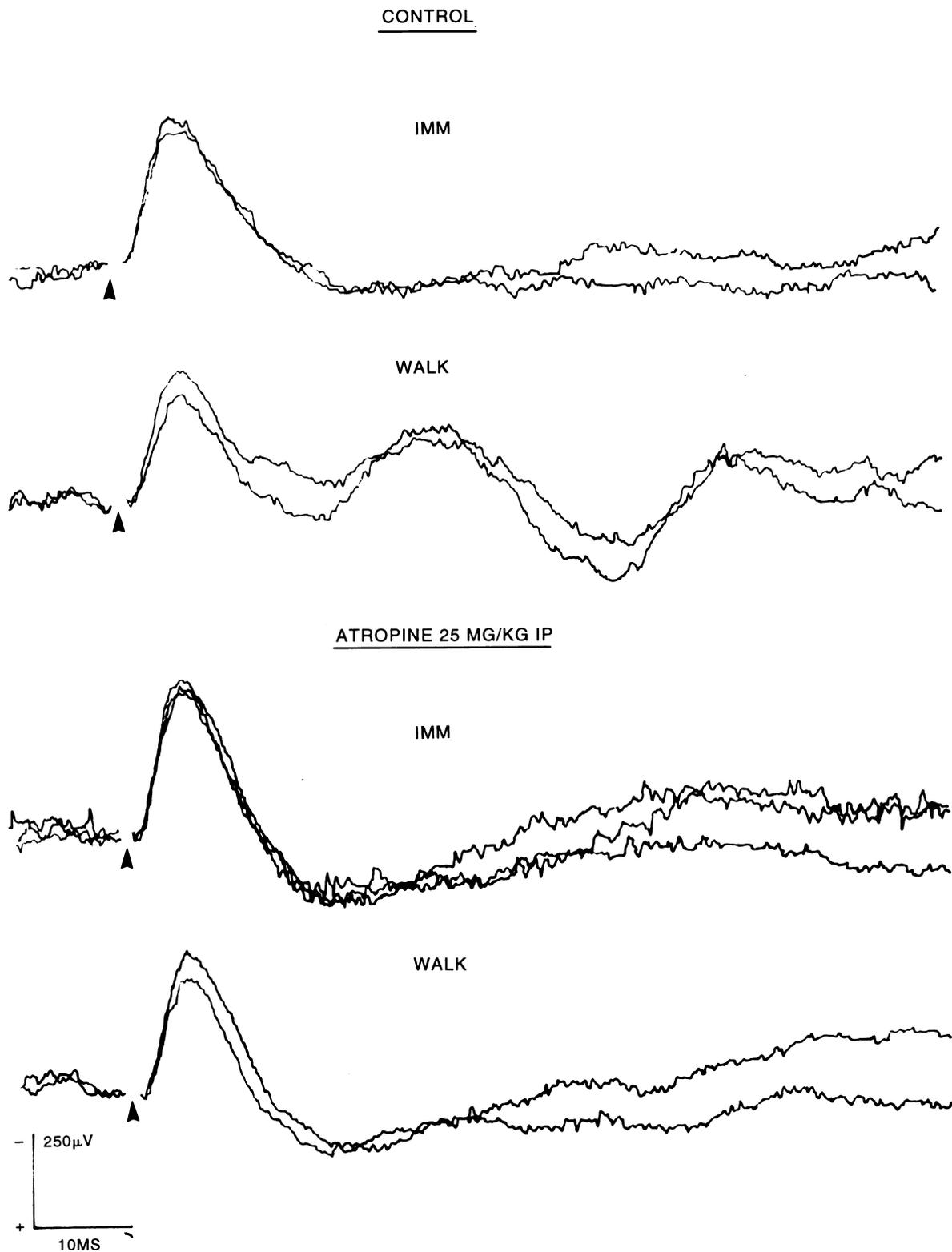
ATROPINE 25 MG/KG IP

IMM

WALK

$-$ | 250μV

$+$

10MS

FIG. 3. Oscillatory Schaffer collateral average evoked potentials were behaviorally dependent and atropine-sensitive. Evoked potentials at the apical dendrites of CA1 were averaged (negative up) after selective stimulation during immobility (IMM) and walking, before and after atropine sulfate (25 mg kg^{-1} i.p.). Note oscillations near 40 Hz during walking, which were abolished by atropine.

Putative interneurons fired phase-locked to the fast waves (18). The fast waves were more pronounced in hippocampal pyramidal cells after Cl$^-$ injection, consistent with GABA$_A$ mediated IPSPs as the underlying mechanism of the fast waves (Fig. 11(C); ref. (88)). After pentobarbital, spontaneous EEG at the 20–70 Hz band was 'pushed' to a lower frequency but a higher power (56), consistent with the action of pentobarbital in increasing the amplitude and
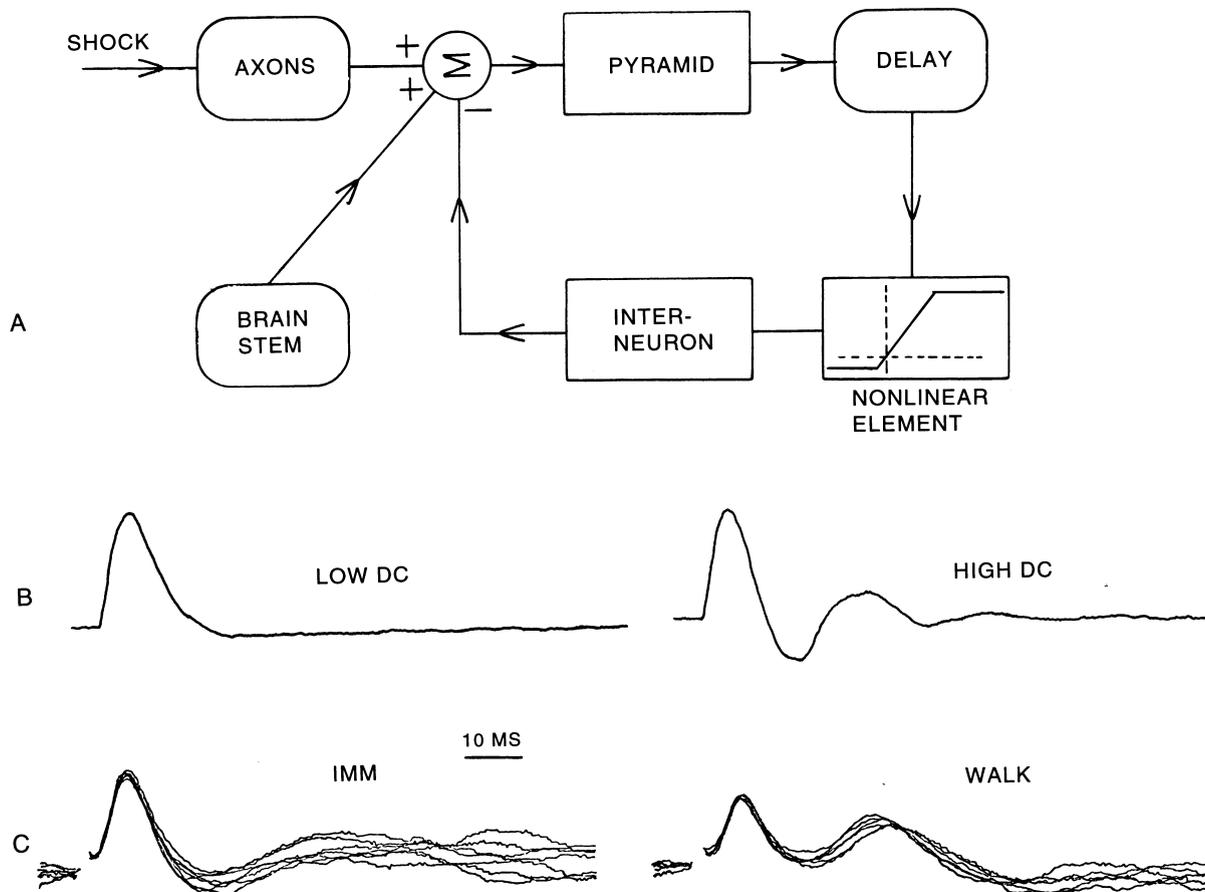
FIG. 4. Model of recurrent inhibition explains the oscillations. (A) Recurrent inhibition (negative feedback) model with a delay and non-linear saturating feedback element through inhibitory interneurons (simplified from ref. (52)). (B) Prediction of the model with low or high brainstem input, which provides a DC bias to the model. (C) Representative experimental data corresponding to immobility (low brainstem input) and walking (high brainstem input).

time course of $GABA_A$ currents; this result could be simulated by the model (52).

The non-linear feedback in the model ((52); Fig. 4) is the critical element that causes oscillation to depend on stimulus intensity. As a consequence of this non-linear feedback, low intensity stimuli evoke oscillations at a relatively higher frequency, and high intensity stimuli evoke oscillations with higher damping and lower frequency. A dependence of the initial IPSP duration on stimulus intensity was shown by Kandel et al. (39) in hippocampal neurons of the anesthetized animal, following various afferent stimulations. Typically, a short IPSP would terminate in a rebound IPSP of the opposite polarity, which was likely caused by a suppression of tonic inhibition (7), i.e. disinhibition predicted by the recurrent inhibition model is manifested intracellularly as the rebound IPSP. The rebound IPSP was found to be associated with an increase in input resistance and reversed at the Cl^- reversal potential like the initial IPSP (7), as expected for a disinhibition.

Recently, Jefferys et al. (38) suggested that metabotropic glutamate receptor activation on hippocampal interneurons may activate rhythmic activities at 40 Hz. A metabotropic glutamate agonist, in the presence of NMDA and non-NMDA glutamate antagonists, induced in CA1 pyramidal cells in vitro a 40 Hz activity. These in vitro oscillations were mediated by $GABA_A$ mediated IPSPs, since they were blocked by bicuculline and slowed by pentobarbital. In the absence of drugs, the pyramidal cell oscillations in vitro could be induced by a tetanus, as has been shown in vivo (57). Jefferys et al. (38) postulated that an interneuronal network was responsible for the in vitro 40 Hz rhythm; recurrent inhibition likely did not exist since the excitation of interneurons by pyramidal cells was blocked by NMDA and non-NMDA antagonists. However, given that pharmacological doses of drugs are needed to induce the in vitro rhythm, and that the physiology in vitro and in vivo are different (below), the physiological relevance of the in vitro 40 Hz rhythm remains to be demonstrated. Evidence cited for an interneuronal network generating fast waves in vivo (38) were considered preliminary (59).

The population spike in the dentate gyrus in response to medial perforant path stimulation was behaviorally dependent (107,108); it was larger in slow-wave sleep than rapid-eye-movement sleep or waking behaviors. Buzsaki et al. (19) reported that the dentate population spike was larger during drinking than running, whereas the commissurally evoked CA1 population spike was larger during running than drinking. The commissurally evoked CA1 population spike was likely evoked by basal dendritic excitation, different from the CA1 spike evoked by apical dendritic excitation (above). On the other hand, the behavioral dependence of the dentate population spike and CA1 apical dendritic population spike was the same—both population spikes were larger during immobility than

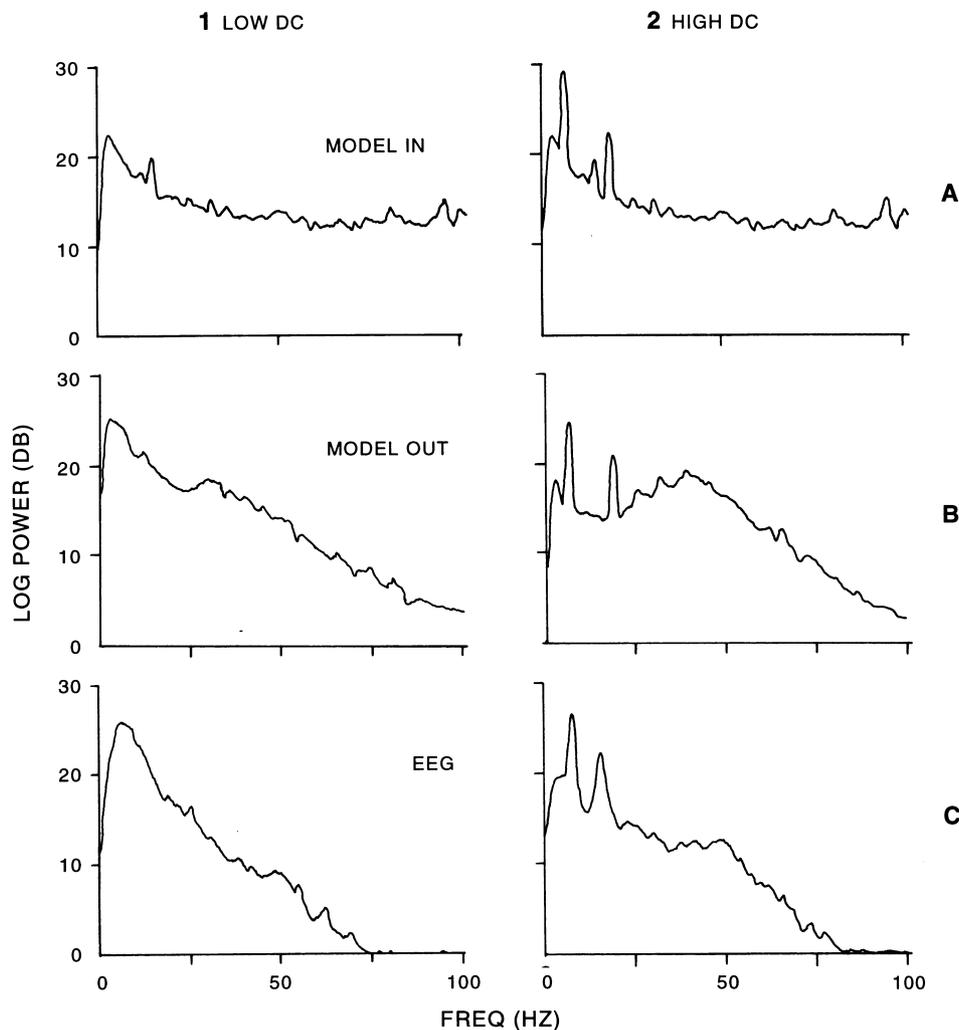**1** LOW DC   **2** HIGH DC

FIG. 5. Model of recurrent inhibition predicts the experimental EEG during presumed low and high DC bias. (A) Power spectra of the Gaussian white-noise input to the model; the brainstem input (DC bias) was not shown in the power spectrum. A 6.3 Hz theta frequency driving was added to the input, on top of the white noise, during the high DC bias (this added theta did not significantly affect EEG responses at other frequencies). (B) Power spectra of the pyramidal cell output of the model, simulating hippocampal EEG. Note the high amplitude of 40 Hz power during a high DC (brainstem input). (C) Experimental EEG power spectra during immobility (presumed low DC) or walking (presumed high DC).

walking and showed similar paired-pulse response dependence (below). The spontaneous fast waves in the hilus of the dentate gyrus of normal rats appeared to be of higher amplitude and frequency than that in CA1 (12,14,17), but oscillatory evoked responses in the dentate gyrus following activation of the perforant path have not been reported.

PAIRED-PULSE RESPONSE IN CA1 AND DENTATE GYRUS

Austin et al. (6) found a robust behavioral dependence of paired-pulse responses in the dentate gyrus following medial perforant path stimulations. We (20) found a similar behavioral dependence of the paired-pulse responses in CA1 following Schaffer collaterals stimulation (Fig. 6). Paired-pulses probe a system in a way that a single pulse could not. The second of a pair of pulses tests the excitability of the neurons at various delays (interpulse intervals, IPIs) after the first pulse perturbs the neural circuit. Paired-pulses reveal mainly a second order of interactions in a system and interaction functions (called kernels) of higher orders in

the dentate gyrus have been estimated by Sclabassi et al. (86). However, the latter technique required monitoring responses to a random pulse train for a long duration (30 min was used). It would be difficult to maintain an animal in a particular behavior for such a long time. In addition, the random pulse train contained brief periods of high frequency pulses capable of eliciting paroxysmal activity, short- or long-term depression/potentiation. Thus, we prefer to deliver a pair of pulses to the animal during a particular behavior.

The most behaviorally sensitive measure of paired-pulse response in CA1 was given by the ratio of the population spikes (i.e. the ratio of the population spike evoked by the second pulse ($P2$) to that evoked by the first pulse ($P1$), or $P2/P1$). The $P2$ versus $P1$ measures of each behavior state tended to cluster together (Fig. 7). While the $P1$ values during immobility and walking may overlap, $P2$ during walking was much larger than that during immobility (30 ms IPI and a low intensity stimulus were used). Similarly, $P2/P1$ was large during rapid-eye-movement sleep
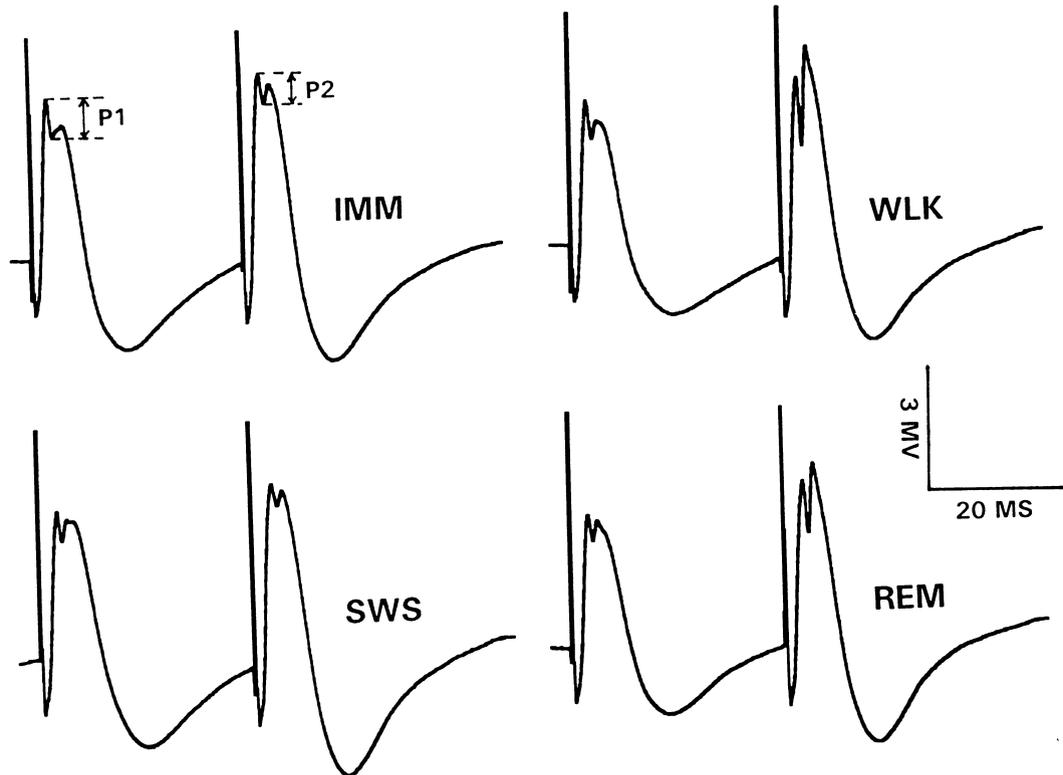
FIG. 6. Paired-pulse responses in the hippocampal CA1 (proximal apical dendrites) following Schaffer collaterals stimulation during different behavioral states (traces are negative up; each trace averaged from eight sweeps). Stimulus intensity was $2 \times$ threshold of the population spike, at an interpulse interval of 30 ms. The second population spike $P2$ was greater than $P1$ during walking (WLK) and rapid-eye-movement sleep (REM), whereas $P2$ was smaller than $P1$ during immobility (IMM) and SWS. Reproduced from ref. (20), with permission.

and small during slow-wave sleep. There was no consistent difference in the $P2/P1$ ratio between walking and rapid-eye-movement sleep, or between immobility and slow-wave sleep (although slow-wave sleep was accompanied by zero $P2$ in this example). $P2/P1$ ratio showed the largest facilitation for low-intensity stimuli and at 30–50 ms IPI (20), corresponding to 20–33 Hz.

Paired-pulse facilitation (PPF) of the Schaffer collateral mediated EPSPs and population spikes in vivo was dependent on stimulus intensity (or the EPSP amplitude). At low stimulus intensities ($< 80 \mu A$), PPF of both EPSP and population spikes was found during all behaviors and under urethane anesthesia. PPF of the EPSPs was likely mediated by presynaptic facilitation (63,113). However, at high intensities ($> 80 \mu A$; IPI of 30–200 ms), the EPSP evoked by the second pulse ($E2$) was smaller than that ($E1$) evoked by the first pulse. As described above, at stimulus intensity that evoked a population spike, $P2$ was smaller than $P1$ during immobility but larger than $P1$ during walking (Fig. 6). Paired-pulse depression of EPSP and population spike at high stimulus intensities may be attributed to inhibition.

Inhibition of the neuronal population may be inferred from measuring the population spike at a fixed population EPSP. The plot of the amplitude of the population spike versus the population EPSP slope revealed a most interesting behavioral relation (Fig. 8) that has not been shown before. During immobility, $P2$ was larger than $P1$ when $P1$ or the EPSP was small, but $P2$ was smaller than $P1$

for a large EPSP or $P1$ (Fig. 8). During walking, both $P2$ and $P1$ increased monontonically with EPSP amplitude (or stimulus intensity), except the $P2$ curve was shifted to the left of the $P1$ curve, i.e. $P2$ was larger than $P1$ at a fixed EPSP (Fig. 8). The upward or leftward shift of the $P2–E2$ curve compared with the $P1–E1$ curve could be interpreted as a removal of inhibition or disinhibition. Muscarinic cholinergic blockade but not serotonin depletion blocked the PPF of population spikes in CA1 during walking (21), suggesting that a cholinergic (medial septal) input is responsible for the disinhibition (47).

The PPF of dentate population spikes (at 20–30 ms IPI) during walking and not during immobility (6) was similar to that in CA1 (20). Preliminary experiments in my laboratory indicate, however, that PPF of the dentate population spikes was not affected by atropine sulfate (25–50 mg kg^{-1} i.p.; Leung and Obasi, unpublished results). Thus, the behaviorally dependent modulation of the dentate population spikes may not be modulated by cholinergic afferents. Bilkey and Goddard (8) also found that the facilitation of spiking in the dentate gyrus following a septal prestimulation was not blocked by an antimuscarinic, although Steffensen et al. (89) found a different result in mice.

Paired-pulse responses in the hippocampal slice in vitro showed properties different from those in vivo. At 50 ms IPI, PPF of EPSPs ($E2 > E1$) and population spikes (i.e. $P2 > P1$) was found at all stimulus intensities in vitro (112), distinct from paired-pulse suppression at high intensity in vivo. Also, population spike facilitation at a fixed EPSP
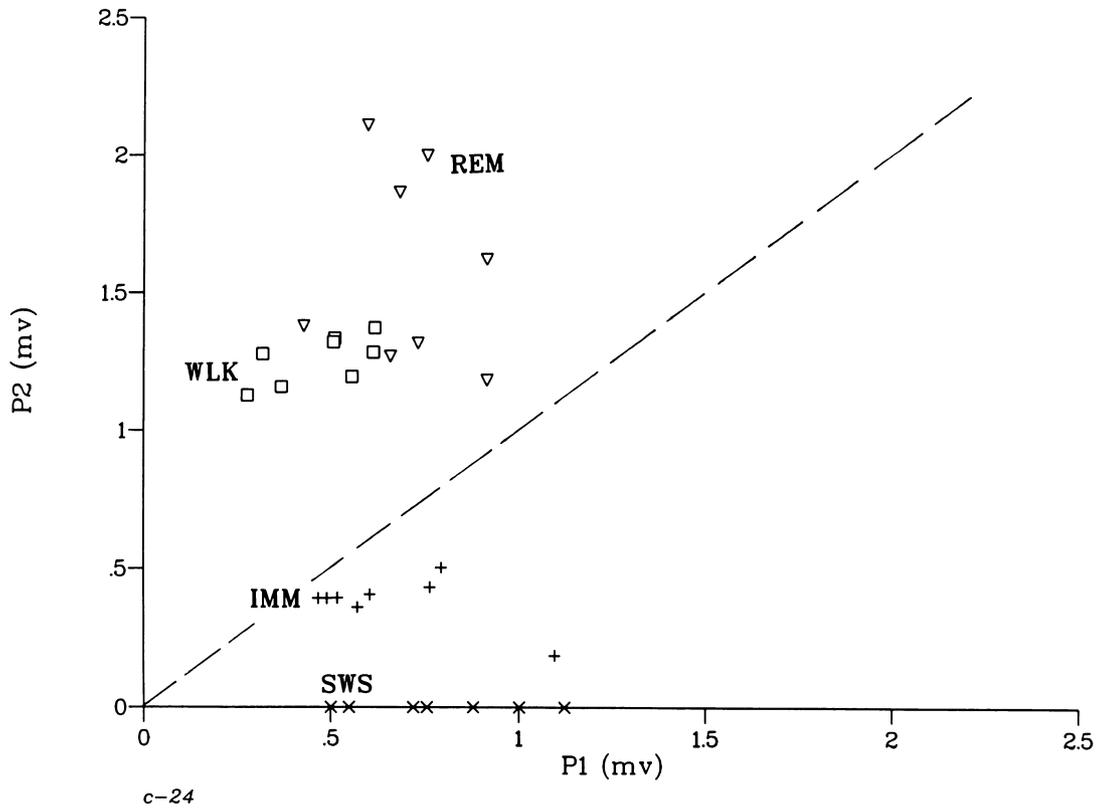
c–24

FIG. 7. The P2 versus P1 plot shows clustering of responses during different behavioral states. P2 and P1 amplitudes were measured for each sweep evoked by Schaffer collateral stimulation (2 × stimulus threshold of the population spike) during four behavioral states: REM, WLK, IMM and SWS. The slanted dashed line is $P2 = P1$.

amplitude was not consistently observed in vitro (63); a small upward shift of P2 compared with P1 was seen at a large EPSP amplitude in the example shown in Fig. 9(A). The population spike threshold in CA1, following Schaffer collateral stimulation, was lower (20–40 μA) in vitro (60) than in vivo (80–200 μA; (84,109)). The lower population spike threshold and its relative lack of paired-pulse depression in vitro suggest that inhibition is lower in vitro than in
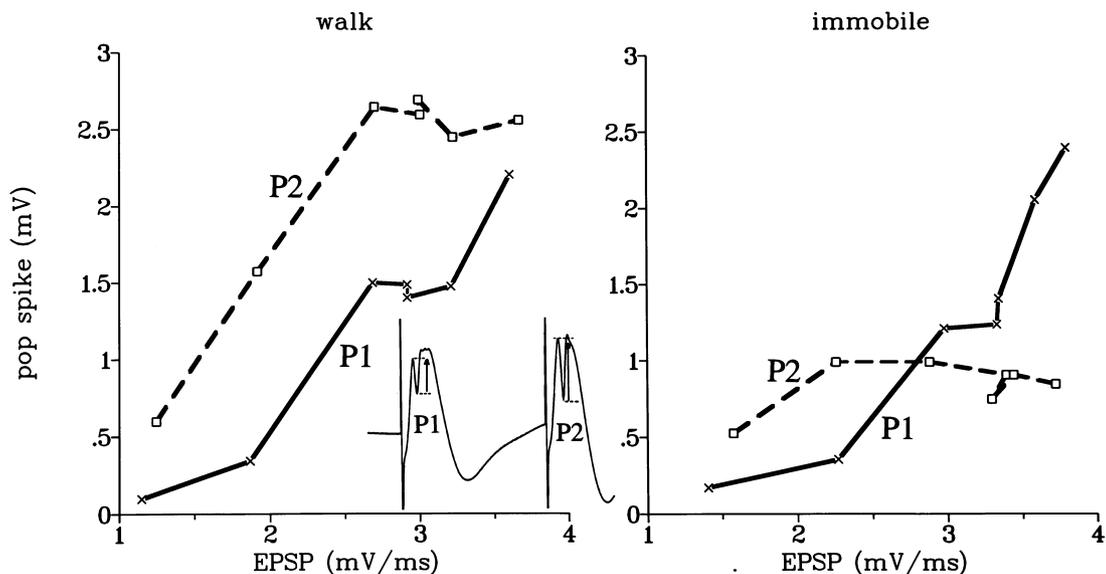

FIG. 8. Plot of population spike amplitude versus EPSP slope in a representative behaving rat. The CA1 responses were recorded in proximal stratum radiatum following paired-pulse stimulation (interpulse interval 30 ms) at the Schaffer collaterals (stratum radiatum) during walking or immobility. For a fixed EPSP, P2 was larger than P1 at all EPSP amplitudes during walking, but P2 was larger than P1 only at a low EPSP during immobility. The graph also shows that P2 (at a fixed EPSP), rather than P1, has a much more robust difference between walk and immobility.
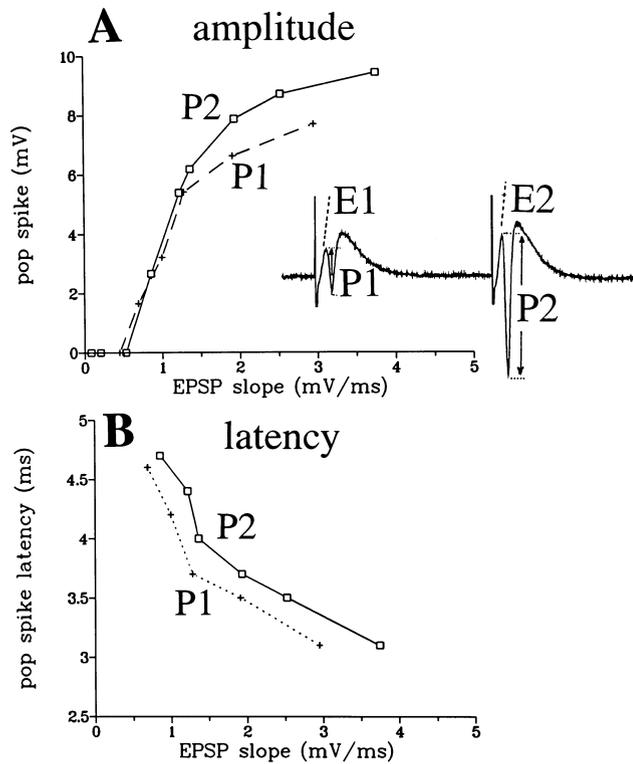
FIG. 9. In vitro (hippocampal slice) spike versus EPSP plots, recorded in CA1 stratum pyramidale, following Schaffer collateral (stratum radiatum) paired-pulse (interpulse interval 50 ms) stimulations. (A) Plot of population spike amplitude versus EPSP slope. The difference in $P2$ and $P1$ amplitudes was small in vitro compared with the behaving rat. (B) Plot of population spike latency versus EPSP slope. The delayed $P2$ peak compared with the $P1$ peak was the same in vitro as in the behaving rat (Fig. 10). $E1$ and $E2$ in the trace in (A) correspond to the EPSP slope following the first and the second pulse, respectively.

vivo. The high tonic IPSP activity in vivo allows more complex dynamic interactions, including acetylcholine-mediated disinhibition during certain behaviors.

In behaving rats (irrespective of behaviors) and in vitro, the $P2$ peak was typically delayed in time compared with the $P1$ peak (Fig. 9(B), Fig. 10). The latter may be interpreted to mean that spikes from different single neurons may arise from a slightly hyperpolarized baseline (during the IPSP evoked by the first pulse), but may fire for a longer time window because of a smaller IPSP evoked by the second pulse (63).

TEMPERATURE EFFECT ON HIPPOCAMPAL EEG AND EVOKED POTENTIALS

Recent experiments suggest that part of the change of hippocampal extracellular potentials may be mediated by a change in brain temperature (2,78). Most of the physiological measures reviewed here varied with the moment-to-moment behavior of the rat, much faster than could be accounted for by the slow change in brain temperature during muscle activity. Presumably, brain temperature during walking should not differ before and after atropine, and yet the evoked potential oscillation and PPF of population spikes during walking was suppressed after atropine. Brain temperature does affect the frequency of the theta rhythm of the behaving rat (104), and various measures of the EPSP and population spike (2).

THETA RHYTHM IN VIVO: EVIDENCE FOR IPSPS AND EPSPS

In anesthetized animals, the theta rhythm showed amplitude peaks at the stratum oriens and stratum radiatum, with
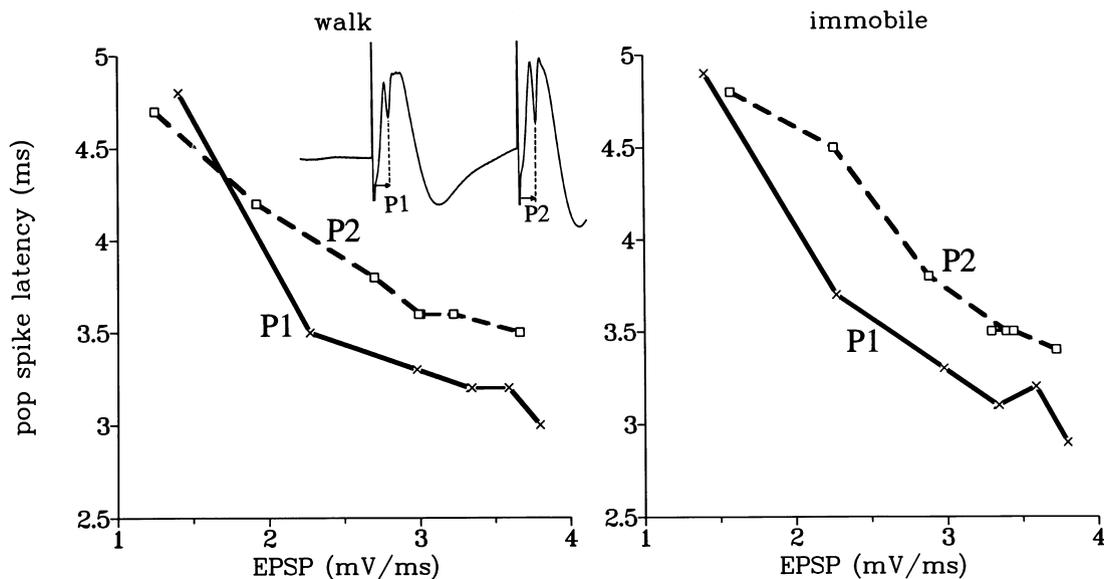

FIG. 10. Plot of population spike latency versus EPSP slope in the behaving rat (same rat as Fig. 8). Peak latency of $P2$ was delayed compared with $P1$, except at very small EPSP, either during walking or immobility.
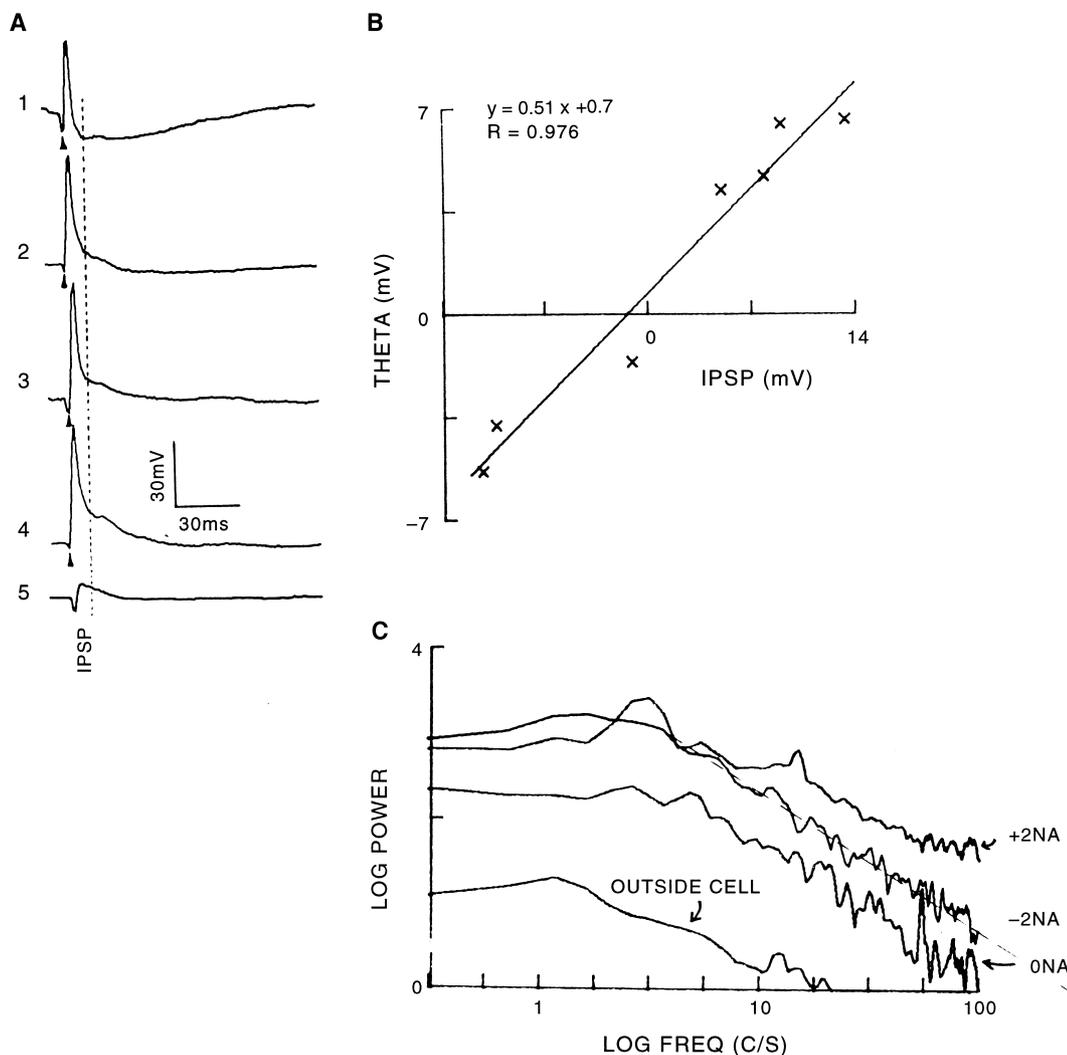
FIG. 11. IPSPs contribute to the theta and gamma-band activity in CA1 neurons in the urethane-anesthetized rat. (A) Averaged alvear evoked antidromic spike and IPSP at different injected currents (± 2 nA). (B) Average peak theta rhythm plotted versus the IPSP amplitude at 10 ms latency (dotted line in (A)); theta was grouped to be either positive or negative depending on the phase shift with respect to the contralateral reference signal. (C) Power spectra (log–log plot) of intracellular spontaneous activity in a CA1 neuron (Leung and Yim, unpublished data, 1986). The power of 10–100 Hz activity increased with the magnitude of the applied current, similar to the change in IPSP amplitude. An approximate first order decay of the gamma power (6 dB/octave; dotted line approximating spectrum of − 2 nA) was found at high frequency. The coherence of the intracellular gamma waves to the reference (extracellular) signal was too low to estimate reliably the phase shift between intra- and extracellular signals. (A) and (B) are from ref. (66), reproduced with permission.

an abrupt phase reversal (180°) near the pyramidal cell layer (12,34). Fox and Ranck (28,82) and Buzsaki et al. (18) have provided evidence that putative interneurons are driven rhythmically at a theta frequency. Artemenko (5) and Fox et al. (29) have provided some evidence that IPSPs partici-pate in an intracellular theta rhythm. The laminar profile of the antidromically evoked IPSP field in CA1 (50) was similar to that of the theta rhythm of anesthetized animals (12,55). In 1983, it seemed that the available information converged on the fact that IPSPs contribute to the theta rhythm, but the definitive experiment was missing. I took the idea that the reversal of IPSPs was the key to the question to K. Krnjević's laboratory, where Conrad Yim and I carried out intracellular recordings from the CA1 cells of urethane-anesthetized rats (65,66). We (65,66) showed that most CA1 cells had intracellular membrane potential oscillations (MPOs) at the theta frequency, and that the MPOs reversed in phase, with respect to the EEG, at a

reversal potential similar to the IPSPs (Fig. 11). The most parsimonious explanation is that the theta rhythm in anesthetized animals consists of a series of rhythmic, somatic IPSPs.

The importance of IPSPs in the generation of the intra-cellularly recorded theta rhythm was confirmed by Fox (27), Soltesz and Deschenes (88) and Ylinen et al. (110). How-ever, there were also conclusions to the contrary. The early work of Fujita and Sato (32) and subsequent work of Nunez et al. (79) claimed that the intracellularly recorded theta rhythm was caused by EPSPs. Two main pieces of evidence were cited for the latter conclusion. First, the intracellular theta rhythm did not reverse with membrane voltage or Cl⁻ injection, and second, the intracellular theta rhythm was larger with hyperpolarization.

With respect to the first piece of evidence, Fujita and Sato (32) claimed that the theta phase did not reverse with Cl⁻ injection, but they had no quantitative assessment of the

phase shift between intra- and extracellular theta rhythms. The only figure shown by Fujita and Sato (32) in support of the lack of theta reversal with Cl⁻ injection apparently showed a depolarization in the initial 25 ms following Schaffer collateral stimulation (their fig. 6A) and they claimed that the IPSP was hyperpolarizing (their Fig. 6B). It may be argued that the IPSP of Fujita and Sato (32) had already been reversed (initially depolarizing) while the late IPSP was still hyperpolarized. Using alvear stimulation which evoked little EPSPs, we found that intracellular theta was phase reversed to the extracellular rhythm when only the initial 10 ms of the IPSP (and not the late IPSP) was reversed by current injection ((66); Fig. 11(A)). Assessment of the reversal of the initial part of the IPSP would be more difficult if it overlapped with an orthodromic EPSP, as in the case of Fujita and Sato (32). A similar lack of quantitative analysis was found in the work of Nunez et al. (79). Although Nunez et al. (79) used a number of cross-correlation techniques in analyzing spike–wave relation, there was no technique to study directly the cross-correlation between intra- or extracellular theta rhythms. Intra- and extracellular waves were averaged by the zero crossing of the extracellular theta, a poor method for the estimate of phase shift at a particular frequency.

With respect to the evidence that the intracellular theta increased with hyperpolarization, this would be expected if either IPSPs or EPSPs were the sole basis of the intracellular rhythm, if the membrane potential is hyperpolarized to a voltage more negative than the IPSP equilibrium potential (normally around −65 mV). Nunez et al. (79) suggested that their impedance measurements, using step currents at various phases of the intracellular theta rhythm, did not reveal an IPSP at a hyperpolarized phase. However, step-impedance measurements during a rhythmic event were difficult to interpret (how could the response to the current pulse be separated from the ongoing rhythm?), and AC impedance measurements using frequencies of up to 100 Hz supported a totally different conclusion (27).

I would suggest that neither Fujita and Sato (32) nor Nunez et al. (79,80) had direct evidence of EPSPs contributing to the intracellular theta. Large intracellular MPO values (up to 30 mV) and excitable cells with a high degree of bursting appeared to be the hallmark of their studies (32,79,80), compared with others (27,66,87,110). The excitable cells probably resulted from the use of curare which antagonized GABA$_A$-mediated IPSPs (48). Thus, IPSPs were smaller in curarized animals and they may be further obscured by excessive spiking. While EPSP was a possible mechanism, there had been no direct proof of this by use of pharmacology (e.g. glutamate antagonists) or physiology (e.g. reversal potential). At a depolarized voltage, intrinsic membrane processes, such as spiking (fast and slow spikes and their afterpotentials) and intrinsic theta-frequency MPOs (below), may be expected to contribute increasingly to the intracellular theta, and this has not been addressed.

THETA RHYTHM IN VIVO: EXTRACELLULAR PROFILE AND MODEL

Theta rhythm in the behaving rat was inferred to consist of atropine-sensitive and atropine-resistant components (10,46,95). The atropine-sensitive component is likely
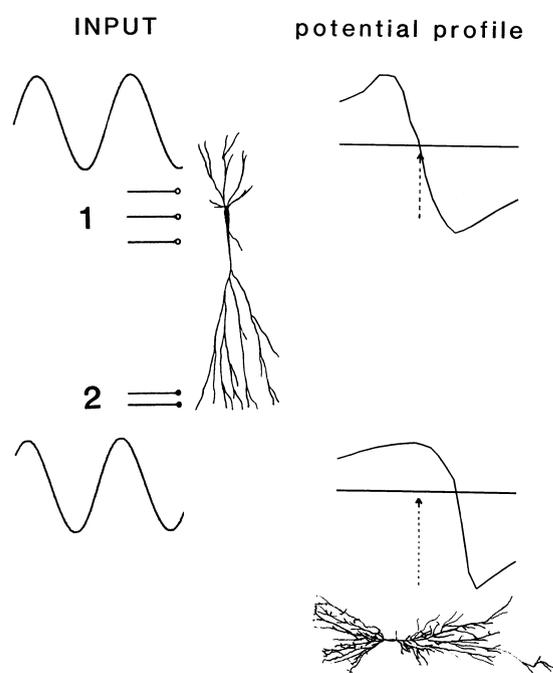

FIG. 12. Two rhythmic drives generating theta rhythm and the gradual phase shift in hippocampal CA1. A proximal input (1) drives the soma and proximal dendrites with inhibitory postsynaptic potentials (via interneurons), resulting in a theta potential profile that shows a dipole field with a reversal at the proximal apical dendrites (proximal stratum radiatum). A distal input (2) drives the distal apical dendrites, presumably with excitatory postsynaptic potentials, resulting in a potential that reverses at the distal apical dendrites. Dotted line with arrow indicates reversal layer of the first dipole field in both potential profiles.

mediated by the cholinergic afferents from the medial septal area while the atropine-resistant component is suggested to be mediated by serotonergic afferents from the raphe (96). Instead of an abrupt phase shift of the theta rhythm in proximal stratum radiatum of urethane-anesthetized (12) or curarized rats (106), Winson (105) found a gradual theta phase reversal (180° over 400 μm) in stratum radiatum in the walking rat. Holsheimer et al. (37) simulated the theta field profiles using a compartment model and concluded that the activation of both pyramidal and granule cells was needed. However, neither the quantitative model of Holsheimer et al. (37) nor the conceptual model of Buzsaki et al. (18) addresses or predicts the gradual theta phase shift in CA1. In 1981, I proposed (in an MRC grant) that the gradual phase shift was caused by the rhythmic driving of two dipole fields with different reversal layers (Fig. 12); the refined model was published in 1984 (55).

A single dipole field was found for the theta rhythm in rats under anesthesia; the dipole was generated by an atropine-sensitive input which generated rhythmic IPSPs. Two dipoles, overlapping in time (phase-shifted) and space (different reversal depths), were inferred for the hippocampal theta rhythm (of different frequencies) during a variety of waking behaviors (53,54). The first dipole was the same as that found under anesthesia and the second dipole was presumably driven by an atropine-resistant input exciting EPSPs at the distal apical dendrites. The atropine-sensitive and atropine-resistant rhythmic drives were phase shifted from each other ((55); Fig. 12), resulting in a gradual theta phase shift in the apical dendritic layer of CA1 (105). In

fact, given the experimental finding of a gradual phase shift in CA1, the theory of extracellular potential generation dictates the necessity of a distal dendritic driving (55).

Synapses on the distal dendrites of CA1 are provided by the entorhinal cortex (4,9,72). In 1984, it was known that some units in the entorhinal cortex fired rhythmically at a theta frequency ((77); subsequent data reviewed by ref. (11)) and that lesion (98) or isolation (99) of the entorhinal cortex removed an atropine-resistant theta input. Administration of atropine did not give a pure dipole field driven by a distal dendritic input (53,55); it may be inferred that atropine only partially blocked the proximal (atropine-sensitive) input, i.e. the proximal driving may not be solely mediated by an atropine-sensitive input. In normal behaving rats, the distal-dendritic theta input apparently does not exist in isolation of the proximal theta input, at least not for durations longer than 1 s (54). Additional support of the distal dendritic driving has been provided by more recent studies. Current source density analysis revealed a rhythmic sink and source pattern at the distal apical dendrites (14,15). Hippocampal theta was attenuated strongly by a selective lesion of cholinergic neurons by saporin-IgG, but the small theta field that remained could be attributed to an atropine-resistant driving of the hippocampus (49). Perforant path inactivation (36) and entorhinal lesion (14) affected the theta amplitude and phase profile in a way consistent with the removal of a distal dendritic driving.

The atropine-sensitive component of the theta rhythm is presumably initiated by the cholinergic cells in the medial septum and diagonal band of Broca (10,81,91) which receive inputs from the brainstem including the supra-mammillary area (40,45,76,101,103). These cholinergic cells may rhythmically drive the hippocampal interneurons (18,55). There is no evidence that the distal dendritic driving is *directly* mediated by a serotonergic input alone (70), but it is possible that a serotonergic input from the raphe (96,100) *or* a cholinergic input may gate the distal dendritic driving, on account of the convergence of cholinergic and serotonergic afferents on hippocampal interneurons in stratum radiatum (30). The driving of the theta rhythm may depend on other neurotransmitters ((11,61,73); glutamate and GABA in the hippocampus have been implicated). In particular, the GABA pathway from the medial septal area to the hippocampus appears to be as large as the cholinergic pathway (42,73), and it may mediate rhythmic driving of the hippocampus, possibly through interneurons (11,44,49,90, 110). The distal, presumed atropine-resistant driving and a small part of the proximal driving of CA1 in the model (55) may come from a septo–hippocampal GABAergic pathway.

Vertes (101) proposed that ''there is only a single theta rhythm of a continuum of frequencies, and that the septohippocampal projection, if not other links in an ascending theta-eliciting system, is cholinergic''. (Vertes now believes that the theta-driving septo–hippocampal projection involves both cholinergic and GABAergic afferents; Vertes, personal communication, 1996). Vertes (101) argued that anticholinergics may penetrate the brain poorly and may not totally block central cholinergic synapses, and a highly activated reticuloseptohippocampal system may drive theta during walking by overriding the partially saturated hippocampal cholinergic receptors. I agree with Vertes with regard to the continuum of theta frequencies driven by a cholinergic theta input—we have inferred that the atropine-sensitive theta input is active during walking (26) and larger with increasing theta frequency. The inference was based on experimental results on CA1-evoked potentials (64) and on phase measurements of the theta rhythm in CA1 (53–55). Apparently, Vertes assumed that the theta during walking was not sufficiently blocked by atropine because large amounts of acetylcholine may be flooding the muscarinic synapses when the reticulo-septohippocampal input was high. Dose response measurement of the phase of the theta phase in stratum radiatum (which was sensitive to atropine) did not reveal any significant change of phase when the dose of atropine was varied tenfold, from 10 to 100 mg kg^{-1} i.p. (53). Furthermore, competition at the muscarinic receptor cannot easily account for the atropine-sensitivity of the theta in rats depleted of serotonin by brainstem lesion or parachloro-phenylalanine or those with the entorhinal cortex isolated (97–100); the theta frequency (up to 10 Hz) and amplitude in these rats were apparently normal before atropine administration. Vertes et al. (102) further argued that a serotonergic input from the median raphe may be desynchronizing as opposed to synchronizing (generating the theta rhythm), but the results were derived from urethane-anesthetized and not behaving rats. Anesthetics have been shown to suppress serotonin effects in the brain (25,35), thus a strong attenuation of the atropine-resistant theta by anesthetics was inferred (46,56). It is possible that serotonergic inputs to the medial septal area mediate some effects on the theta rhythm (91), and these effects need to be further studied, but serotonergic inputs may also affect hippocampal theta via a pathway through the entorhinal cortex (55,98,99).

The effect of a distal dendritic driving on modulating hippocampal response is unclear. After blocking the atropine-sensitive afferents by atropine or scopolamine, the behavioral dependence of Schaffer collateral evoked response in CA1 was strongly attenuated (21,64), suggesting only a weak modulation of evoked synaptic transmission by the atropine-resistant afferents alone. Furthermore, while serotonin depletion by parachlorophenylalanine increased the occurrence of theta during immobility, it had no apparent effect on the peak theta rhythm during walking (70,97) or the CA1 theta phase profile during walking (70). Serotonin depletion also appeared to have no effect on the evoked response in CA1 or its correlation with behavior (21). Nor did serotonin depletion have any significant effect on the behavior of a rat (97). It has been suggested that serotonin may provide a redundant effect which may be obscured by the presence of a cholinergic afferents (70), or the depletion of serotonin exacerbate the physiological and behavioral effects of cholinergic blockade. The lack of a theta rhythm and the severe impairment of behavior in rats depleted of serotonin and given muscarinic antagonists (83,97) supports this suggestion.

In summary, I conclude that the assumptions of atropine-sensitive and atropine-resistant components of the hippocampal theta rhythm are well founded, and the model of how these inputs drive hippocampal theta (55) has been confirmed in general. However, how serotonergic inputs drive or enable a theta rhythm, how a septohippocampal GABA input participates in the theta generation, and how an atropine-resistant input may affect physiological processing and behavioral function are questions that need to be further studied.

THETA RHYTHM GENERATION IN VITRO

The hippocampal slice in vitro, with normal artificial cerebrospinal fluid, had little spontaneous activity. Konopacki et al. ((43); reviewed in (11)) first demonstrated that perfusion of carbachol induced periods of theta-frequency oscillations in the hippocampus in vitro. This was confirmed by MacVicar and Tse (75) in CA3, who also showed that the carbachol-induced rhythm in vitro was apparently synaptically generated, and that it could be abolished by tetrodotoxin (75). Carbachol may induce similar field potential rhythm in anesthetized rats (85) but the combination of bicuculline and carbachol may be necessary to induce the rhythm in behaving animals (24). The fact that carbachol may induce a theta-frequency oscillations in the hippocampal slice, isolated from other subcortical inputs, suggests that intrinsic activity in the hippocampus may be responsible for generating the theta rhythmicity.

The carbachol results do not necessarily imply a capability of oscillations in single hippocampal neurons. Leung and Yim (67,68) reported intrinsic theta-frequency MPOs that were induced in hippocampal neurons solely by depolarization (Fig. 13), even in the absence of synaptic transmission (68,74). The hippocampal MPOs normally depended on a low-threshold persistent sodium current (68,74) and a potassium current that was sensitive to tetraethylammonium (33,68). If the low-threshold sodium current was blocked by tetrodotoxin or the local anesthetic QX314, contribution of a high-threshold calcium current to the MPOs may also be revealed (68). MPOs with similar frequencies and characteristics were found in layer II cells of the entorhinal cortex (1,41). Depolarization-induced single neuronal MPOs may contribute to the spontaneous carbachol-induced field rhythm (67).

Systems analysis tells us that if a system shows a spontaneous rhythm of a particular frequency, it will also resonate (or respond maximally) to an almost identical frequency. Enhanced response to driving at the theta frequency has been demonstrated independently by Garcia-Monoz et al. (33) and our laboratory ((111); Leung and Yu, in preparation). A CA1 neuron of resting membrane potential more depolarized than about -60 mV could be driven preferentially by sine wave currents within a limited range of the theta frequency (not shown). The latter is the resonance phenomenon in CA1 neurons and it often appears to be more robust than the spontaneous MPOs. This result embodies the condition underlying theta generation in the behaving animal, in which intrinsic voltage-dependent processes modulate the extrinsic rhythmic driving by the medial septal area. The coordination between extrinsic and intrinsic mechanisms of rhythm generation has been demonstrated by Cobb et al. (23), who showed that rhythmic driving of individual inhibitory interneurons could synchronize the theta-frequency MPOs of many pyramidal cells in vitro. Thus, the extrinsic drive serves to synchronize large areas of the brain, and the intrinsic processes serve to veto (disrupt) or enhance the extrinsic driving.

I still favor the medial septal (and diagonal band of Broca) neurons as the primary pacemakers of theta rhythmicity, thus synchronizing the many forebrain structures (11), including the hippocampus bilaterally, entorhinal (77) and posterior cingulate cortex (13,62). The intrinsic conductances may amplify or attenuate the driving. I do not favor intrinsic local processes as the primary cause of theta rhythmicity in the hippocampus in vivo for two main reasons.

1. The intrinsic rhythm in a single cell tended not to be highly regular and, in our experience, the carbachol-induced rhythm in vitro was not persistent or consistent across slices or cells (67).
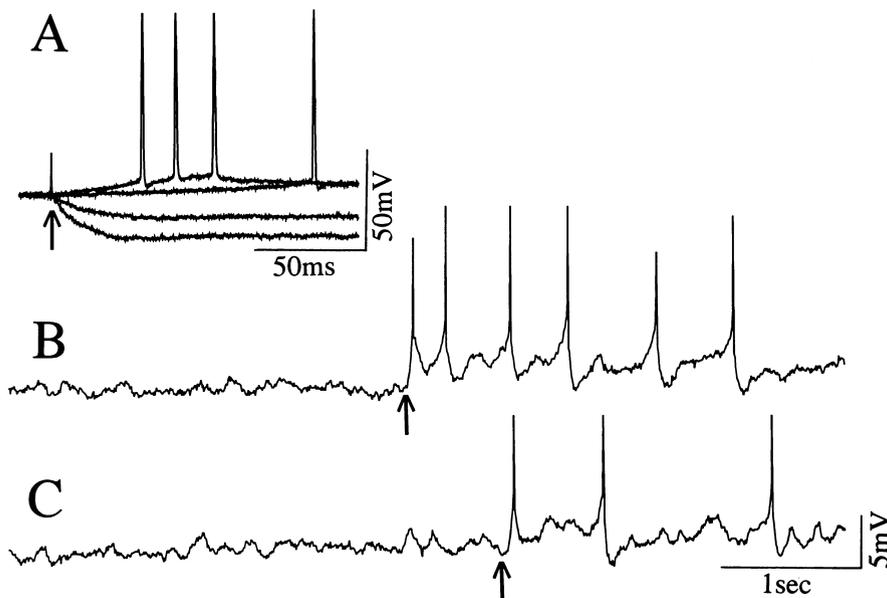

FIG. 13. Membrane potential oscillations (MPOs) were induced by depolarizing currents in hippocampal CA1 neurons in the slice in vitro. (A) Fast sweep to show responses to hyperpolarizing and depolarizing current steps. (B) and (C) Slow sweep to show MPOs induced during the step of a current (arrow) of 0.1 nA (B) or 0.05 nA (C).

2. The induction of population rhythm by cholinergic agonists in vitro (11,43,67) and especially in animals (24) appears to require conditions that are not physiological.

In conclusion, my quest to understand the 'theta state' is still not completed. However, as reviewed here, the use of systems analysis in vitro and in behaving rats has opened up new insights and avenues in the study of hippocampal rhythm generation.

REFERENCES

1. Alonso, A. and Llinas, R. R., Subthreshold Na$^+$-dependent theta-like rhythmicity in entorhinal cortex layer II stellate cells. *Nature*, 1989, **342**, 175–177.

2. Andersen, P. and Moser, E. I., Brain temperature and hippocampal function. *Hippocampus*, 1995, **5**, 491–498.

3. Andersen, P., Bliss, T. V. P. and Skrede, K. K., Unit analysis of hippocampal population spikes. *Experimental Brain Research*, 1971, **13**, 208–221.

4. Andersen, P., Holmqvist, B. and Voorhoeve, P. E., Excitatory synapses on hippocampal apical dendrites activated by entorhinal stimulation. *Acta Physiologica Scandinavica*, 1966, **66**, 461–472.

5. Artemenko, D. P., Role of hippocampal neurons in theta-wave generation. *Neurophysiology*, 1973, **4**, 409–415.

6. Austin, K. B., Bronzino, J. D. and Morgane, P. J., Pair-pulse facilitation and inhibition in the dentate gyrus is dependent on behavioral state. *Experimental Brain Research*, 1989, **77**, 594–604.

7. Ben-Ari, Y., Krnjevic, K., Reiffenstein, R. J. and Reinhardt, W., Inhibitory conductance changes and action of gamma-aminobutyrate in rat hippocampus. *Neuroscience*, 1981, **6**, 2445–2463.

8. Bilkey, D. K. and Goddard, G. V., Medial septal facilitation of hippocampal granule cell activity is mediated by inhibition of inhibitory interneurons. *Brain Research*, 1985, **361**, 99–106.

9. Blackstad, T. W., On the termination of some afferents to the hippocampus and fascia dentata. *Acta Anatomica*, 1958, **35**, 202–214.

10. Bland, B. H., The physiology and pharmacology of hippocampal formation theta rhythms. *Progress in Neurobiology*, 1986, **26**, 1–54.

11. Bland, B. H. and Colom, L. V., The physiology and pharmacology of hippocampal formation theta rhythms. *Progress in Neurobiology*, 1993, **41**, 157–208.

12. Bland, B. H. and Whishaw, I. Q., Generators and topography of hippocampal theta (RSA) in the anaesthetized and freely moving rat. *Brain Research*, 1976, **118**, 259–280.

13. Borst, J. G. G., Leung, L.-W. S. and MacFabe, D. F., Electrical activity in the cingulate cortex of the rat. II. Cholinergic modulation. *Brain Research*, 1987, **407**, 81–93.

14. Bragin, A., Jando, G., Nadasdy, Z., Hetke, J., Wise, K. and Buzsaki, G., Gamma (40–100 Hz) oscillation in the hippocampus of the behaving rat. *Journal of Neuroscience*, 1995, **15**, 47–60.

15. Brankack, J., Stewart, M. and Fox, S. E., Current source density analysis of the hippocampal theta rhythm: associated sustained potentials and candidate synaptic generators. *Brain Research*, 1993, **615**, 310–327.

16. Bressler, S. L., The gamma wave: A cortical information carrier? *Trends in Neuroscience*, 1990, **13**, 161–162.

17. Buzsaki, G., Generation of hippocampal EEG patterns. In The Hippocampus, Vol. 3, ed. R. L. Isaacson and K. H. Pribram. Plenum Press, New York, 1986, pp. 137–168.

18. Buzsaki, G., Leung, L. S. and Vanderwolf, C. H., Cellular bases of hippocampal EEG in the behaving rat. *Brain Research Reviews*, 1983, **6**, 139–171.

19. Buzsaki, G., Grastyan, E., Czopf, J., Kellenyi, L. and Prohaska, O., Changes in neuronal transmission in the rat hippocampus during behavior. *Brain Research*, 1981, **225**, 235–247.

20. Cao, F. and Leung, L. S., Behavior-dependent paired pulse responses in the hippocampal CA1 region. *Experimental Brain Research*, 1991, **87**, 553–561.

21. Cao, F. and Leung, L. S., Effect of atropine and PCPA on the behavioral modulation of paired-pulse response in the hippocampal CA1 region. *Brain Research*, 1992, **576**, 339–342.

22. Ciba Foundation Symposium 58. Functions of the Septo–hippocampal System. Elsevier, Amsterdam, 1978, 446 pp.

23. Cobb, S. R., Buhl, E. H., Halasy, K., Paulsen, O. and Somogyi, P., Synchronization of neuronal activity in hippocampus by individual GABAergic interneurons. *Nature*, 1995, **378**, 75–78.

24. Colom, L. V., Nassif-Caudarella, S., Dickson, C. T., Smythe, J. W. and Bland, B. H., In vivo intrahippocampal microfusion of carbachol and bicuculline induces theta-like oscillations in the septally deafferented hippocampus. *Hippocampus*, 1991, **1**, 381–390.

25. Dringeberg, H. C. and Vanderwolf, C. H., Some general anesthetics reduce serotonergic neocortical activation and enhance the action of serotonergic antagonists. *Brain Research Bulletin*, 1995, **36**, 285–292.

26. Dudar, J. D., Whishaw, I. Q. and Szerb, J. C., Release of acetylcholine from the hippocampus of freely moving rats during sensory stimulation and running. *Neuropharmacology*, 1979, **18**, 673–678.

27. Fox, S. E., Membrane potential and impedance changes in hippocampal pyramidal cells during theta rhythm. *Experimental Brain Research*, 1989, **77**, 283–294.

28. Fox, S. E. and Ranck, J. B. Jr., Localization and anatomical identification of theta and complex spike cells in dorsal hippocampal formation of rats. *Experimental Neurology*, 1975, **49**, 299–313.

29. Fox, S. E., Wolfson, S. and Ranck, J. B., Jr., Investigating the mechanisms of hippocampal theta rhythms: Approaches and progress. In Neurobiology of the Hippocampus, ed. W. Siefert. Academic Press, New York, 1983, pp. 303–319.

30. Freund, T. F., Gulyas, A. I., Acsady, L. L., Gorcs, T. and Toth, K., Serotonergic control of the hippocampus via local inhibitory interneurons. *Proceedings of the National Academy of Sciences of the United States of America*, 1990, **87**, 8501–8505.

31. Freeman, W. J., Mass Action in the Nervous System. Academic Press, New York, 1975.

32. Fujita, Y. and Sato, T., Intracellular records from hippocampal pyramidal cells in rabbit during theta rhythm activity. *Journal of Neurophysiology*, 1964, **27**, 1011–1025.

33. Garcia-Monz, A., Barrio, L. C. and Buno, W., Membrane potential oscillations in CA1 hippocampal pyramidal neurons *in vitro*: intrinsic rhythms and fluctuations entrained by sinusoidal injected current. *Experimental Brain Research*, 1993, **97**, 325–333.

34. Green, J. D., Maxwell, D. S., Schindler, W. and Stumpf, C., Rabbit EEG 'theta' rhythm: its anatomical source and relation to activity in single neurons. *Journal of Neurophysiology*, 1960, **23**, 403–420.

35. Heym, J., Steinfels, G. F. and Jacobs, B. L., Choral hydrate anesthesia alters the responsiveness of central serotonergic neurons in the cat. *Brain Research*, 1984, **291**, 63–72.

36. Heynen, A. J. and Bilkey, D. K., Effects of perforant path procaine on hippocampal type 2 rhythmical slow-wave activity (theta) in the urethane-anesthetized rat. *Hippocampus*, 1994, **4**, 683–695.

37. Holsheimer, J., Boers, J., Lopes da Silva, F. H. and van Rotterdam, A., The double dipole model of theta rhythm generation: simulation

of laminar field potential profiles in the rat hippocampus. *Brain Research*, 1982, **235**, 31–50.

38. Jefferys, J. G. R., Traub, R. D. and Whittington, M. A., Neuronal networks for induced '40 Hz' rhythms. *Trends in Neuroscience*, 1996, **19**, 202–208.

39. Kandel, E. R., Spencer, W. A. and Brinley, F. J. Jr., Electrophysiology of hippocampal neurons. I. Sequential invasion and synaptic organization. *Journal of Neurophysiology*, 1961, **24**, 225–242.

40. Kirk, I. J., Oddie, S. D., Konopacki, J. and Bland, B. H., Evidence for differential control of posterior hypothalamic, supramammillary, and medial mammillary theta-related cellular discharge by ascending and descending pathways. *Journal of Neuroscience*, 1996, **16**, 5547–5554.

41. Klink, R. and Alonso, A., Ionic mechanisms for the subthreshold oscillations and differential electroresponsiveness of medial entorhinal cortex layer—II Neurons. *Journal of Neurophysiology*, 1993, **70**, 144–157.

42. Kohler, C., Chan-Palay, V. and Wu, J.-Y., Septal neurons containing glutamic acid decarboxylase immunoreactivity project to the hippocampal region in the rat brain. *Anatomy and Embryology*, 1984, **169**, 41–44.

43. Konopacki, J., MacIver, M. B., Bland, B. H. and Roth, S. H., Carbachol-induced EEG 'theta' activity in hippocampal brain slices. *Brain Research*, 1987, **405**, 196–198.

44. Konopacki, J., Bland, B. H., Colom, L. V. and Oddie, S. D., In vivo intracellular correlates of hippocampal formation theta-on and theta-off cells. *Brain Research*, 1992, **586**, 247–255.

45. Kocsis, B. and Vertes, R. P., Characterization of neurons in the supramammillary nucleus and mammillary body that discharge rhythmically with the hippocampal theta rhythm in the rat. *Journal of Neuroscience*, 1994, **14**, 7040–7052.

46. Kramis, R. C., Vanderwolf, C. H. and Bland, B. H., Two types of hippocampal rhythmical slow activity in both the rabbit and the rat: Relations to behavior and effects of atropine, diethyl ether, urethane and pentobarbital. *Experimental Neurology*, 1975, **49**, 58–85.

47. Krnjević, K., Ropert, N. and Casullo, J., Septohippocampal disinhibition. *Brain Research*, 1988, **438**, 182–192.

48. Lebeda, F. J., Hablitz, J. J. and Johnston, D., Antagonism of GABA-mediated responses by d-tubocurarine in hippocampal neurons. *Journal of Neurophysiology*, 1982, **48**, 622–632.

49. Lee, M. G., Chrobak, J. J., Sik, A., Wiley, R. G. and Buzsaki, G., Hippocampal theta activity following selective lesion of the septal cholinergic system. *Neuroscience*, 1994, **62**, 1033–1047.

50. Leung, L. S., Potentials evoked by the alvear tract in hippocampal CA1 of rats II. Spatial field analysis. *Journal of Neurophysiology*, 1979, **42**, 1571–1589.

51. Leung, L. S., Behavior-dependent evoked potentials in the hippocampal CA1 region of the rat. I Correlation with behavior and EEG. *Brain Research*, 1980, **198**, 95–117.

52. Leung, L. S., Nonlinear feedback model of neuronal populations in the hippocampal CA1 region. *Journal of Neurophysiology*, 1982, **47**, 845–868.

53. Leung, L. S., Pharmacology of theta phase shift in the hippocampal CA1 region of freely moving rats. *Electroencephalography and Clinical Neurophysiology*, 1984, **58**, 457–466.

54. Leung, L. S., Theta rhythm during REM sleep and waking: correlations between power, phase and frequency. *Electroencephalography and Clinical Neurophysiology*, 1984, **58**, 553–564.

55. Leung, L. S., Model of gradual phase shift of theta rhythm in the rat. *Journal of Neurophysiology*, 1984, **52**, 1051–1065.

56. Leung, L. S., Spectral analysis of hippocampal EEG in the freely moving rat: effects of centrally active drugs and relations to evoked potentials. *Electroencephalography and Clinical Neurophysiology*, 1985, **60**, 65–77.

57. Leung, L. S., Hippocampal electrical activity following local tetanization I. Afterdischarges. *Brain Research*, 1987, **419**, 173–187.

58. Leung, L. S., The hippocampal fast (Beta) rhythm—a review. *Hippocampus*, 1992, **2**, 93–98.

59. Leung, L. S., Recurrent inhibition model of hippocampal CA1 in vivo. *Trends in Neuroscience*, 1996, **19**, 468–469.

60. Leung, L. S. and Au, A. S., Long-term potentiation as a function of test pulse intensity: a study using input/output profiles. *Brain Research Bulletin*, 1994, **33**, 453–460.

61. Leung, L. S. and Desborough, K. A., APV, an *N*-methyl-D-aspartate receptor antagonist, blocks the hippocampal theta rhythm in behaving rats. *Brain Research*, 1988, **463**, 148–152.

62. Leung, L. S. and Borst, J. G.G., Electrical activity in the cingulate cortex of the rat. I. Generating mechanisms and relations to behavior. *Brain Research*, 1987, **407**, 68–80.

63. Leung, L. S. and Fu, X.-W., Factors affecting paired-pulse facilitation in CA1 neurons in vitro. *Brain Research*, 1994, **650**, 75–84.

64. Leung, L. S. and Vanderwolf, C. H., Behavior-dependent evoked potentials in the hippocampal CA1 region of the rat. II. Effect of eserine, atropine, ether and pentobarbital. *Brain Research*, 1980, **198**, 119–133.

65. Leung, L. S. and Yim, C. Y., Intracellular records of theta rhythm in hippocampal CA1 cells of the rat. *Proceedings of the Canadian Federal Biological Society*, 1984, **27**, 40.

66. Leung, L. S. and Yim, C. Y., Intracellular records of theta rhythm in hippocampal CA1 cells of the rat. *Brain Research*, 1986, **367**, 323–327.

67. Leung, L. S. and Yim, C. Y., Membrane potential oscillations in hippocampal neurons induced by carbachol or depolarizing currents. *Neuroscience Research Communications*, 1988, **2**, 159–167.

68. Leung, L. S. and Yim, C. Y., Intrinsic membrane potential oscillations in hippocampal neurons in vitro. *Brain Research*, 1991, **553**, 261–274.

69. Leung, L. S., Lopes da Silva, F. H. and Wadman, W. J., Spectral characteristics of the hippocampal EEG in the freely moving rat. *Electroencephalography and Clinical Neurophysiology*, 1982, **54**, 203–219.

70. Leung, L. S., Martin, L. and Stewart, D. J., Hippocampal theta rhythm in behaving rats following ibotenic acid lesion of the septum. *Hippocampus*, 1994, **4**, 136–147.

71. Leung, L. S., Msi, V. and Desborough, K. A., Hippocampal electrical activity in the Brattleboro rat. *Experimental Neurology*, 1987, **97**, 672–685.

72. Leung, L. S., Roth, L. and Canning, K., Entorhinal inputs to the hippocampal CA1 and dentate gyrus in the rat: a current-source–density study. *Journal of Neurophysiology*, 1995, **73**, 2392–2403.

73. Lopes da Silva, F. H., Witter, M. P., Boeijinga, P. H. and Lothman, A. H.M., Anatomic organization and physiology of the limbic cortex. *Physiological Reviews*, 1990, **70**, 453–511.

74. MacVicar, B. A., Depolarizing prepotentials are Na^+ dependent in CA1 pyramidal neurons. *Brain Research*, 1985, **333**, 378–381.

75. MacVicar, B. A. and Tse, F. W. Y., Local neuronal circuitry underlying cholinergic rhythmical slow activity in CA3 area of rat hippocampal slices. *Journal of Physiology (London)*, 1989, **417**, 197–212.

76. McNaughton, N., Logan, B., Panickar, K. S., Kirk, I. J., Pan, W. X., Brown, N. T. and Heenan, A., Contribution of synapses in the medial supramammillary nucleus to the frequency of hippocampal theta rhythm in freely moving rats. *Hippocampus*, 1995, **5**, 534–545.

77. Mitchell, S. J. and Ranck, J. B. Jr., Generation of theta rhythm in medial entorhinal cortex of freely moving rat. *Brain Research*, 1980, **189**, 49–66.

78. Moser, E., Mathiesen, I. and Andersen, P., Association between brain temperature and dentate field potentials in exploring and swimming rats. *Science*, 1993, **259**, 1324–1326.

79. Nunez, A., Garcia-Austt, E. and Buno, W. Jr., Intracellular theta-rhythm generation in identified hippocampal pyramids. *Brain Research*, 1987, **416**, 289–300.

80. Nunez, A., Garcia-Austt, E. and Buno, W. Jr., Synaptic contributions to theta rhythm genesis in rat CA1–CA3 hippocampal pyramidal neurons in vivo. *Brain Research*, 1990, **533**, 176–179.

81. Petsche, H., Stumpf, C. and Gogolak, G., The significance of the rabbit's septum as a relay station between the midbrain and the hippocampus. I. The control of hippocampal arousal activity by the septum cells. *Electroencephalography and Clinical Neurophysiology*, 1962, **14**, 202–211.

82. Ranck, J. B. Jr., Studies of single neurons in dorsal hippocampal formation and septum in unrestrained rats. Part I. Behavioral correlates and firing repertoires. *Experimental Neurology*, 1973, **41**, 461–531.

83. Richterlevin, G., Greenberger, V. and Segal, M., The effects of general and restricted serotonergic lesions on hippocampal electrophysiology and behavior. *Brain Research*, 1994, **642**, 111–116.

84. Roth, L. R. and Leung, L. S., Difference in LTP at the basal and apical dendrites of CA1 pyramidal neurons in urethane-anesthetized rats. *Brain Research*, 1995, **694**, 40–48.

85. Rowntree, C. I. and Bland, B. H., An analysis of cholinoceptive neurons in the hippocampal formation by direct microinfusion. *Brain Research*, 1986, **362**, 98–113.

86. Sclabassi, R. J., Ericksson, J. L., Port, R. L., Robinson, G. B. and Berger, T. W., Nonlinear systems analysis of the hippocampal perforant path-dentate projection I. Theoretical and interpretational considerations. *Journal of Neurophysiology*, 1988, **60**, 1066–1076.

87. Singer, W., Synchronization of cortical activity and its putative role in information processing and learning. *Annual Review of Physiology*, 1993, **55**, 349–374.

88. Soltesz, I. and Deschenes, M., Low- and high-frequency membrane potential oscillations during theta activity in CA1 and CA3 pyramidal neurons of the rat hippocampus under ketamine–xylazine anesthesia. *Journal of Neurophysiology*, 1993, **70**, 97–116.

89. Steffensen, S. C., Campbell, I. L. and Henriksen, S. J., Site-specific hippocampal pathophysiology due to cerebral overexpression of interleukin-6 in transgenic mice. *Brain Research*, 1994, **652**, 149–153.

90. Stewart, M. and Fox, S. E., Detection of an atropine-resistant component of hippocampal theta rhythm in urethane-anesthetized rats. *Brain Research*, 1989, **500**, 55–60.

91. Stewart, M. and Fox, S. E., Do septal neurons pace the hippocampal theta rhythm?. *Trends in Neuroscience*, 1990, **13**, 163–168.

92. Stumpf, C., Drug action on the electrical activity of the hippocampus. *International Review of Neurobiology*, 1965, **8**, 77–138.

93. Stumpf, C., The fast component in the electrical activity of rabbit's hippocampus. *Electroencephalography and Clinical Neurophysiology*, 1965, **18**, 477–486.

94. Vanderwolf, C. H., Hippocampal electrical activity and voluntary movement in the rat. *Electroencephalography and Clinical Neurophysiology*, 1969, **26**, 407–418.

95. Vanderwolf, C. H., Neocortical and hippocampal activation in relation to behavior: effects of atropine, eserine, phenothiazines, and amphetamine. *Journal of Comparative Physiology and Psychology*, 1975, **88**, 300–323.

96. Vanderwolf, C. H., Cerebral activity and behavior: control by cholinergic and serotonergic systems. *International Review of Neurobiology*, 1988, **30**, 225–340.

97. Vanderwolf, C. H. and Baker, G., Evidence that serotonin mediates non-cholinergic low-voltage fast activity, non-cholinergic hippocampal rhythmical slow activity and cognitive abilities. *Brain Research*, 1986, **374**, 342–356.

98. Vanderwolf, C. H. and Leung, L.-W. S., Hippocampal rhythmical slow activity: A brief history and the effects of entorhinal lesions and phencyclidine. In Neurobiology of the Hippocampus, ed. G. Siefert. Academic Press, London, 1983, pp. 275–302.

99. Vanderwolf, C. H., Leung, L.-W. S. and Cooley, R. K., Pathways through the cingulate, neo- and entorhinal cortices mediating atropine-resistant hippocampal rhythmical slow activity. *Brain Research*, 1985, **347**, 58–73.

100. Vanderwolf, C. H., Leung, L. W.S., Baker, G. B. and Stewart, D. J., The role of serotonin in the control of cerebral activity: studies with intra-cerebral 5,7-dihydroxytryptamine. *Brain Research*, 1989, **504**, 181–191.

101. Vertes, R. P., Brainstem modulation of the hippocampus. In The Hippocampus, Vol. 4, ed. R. L. Isaacson and K. H. Pribram. Plenum Press, New York, 1986, pp. 41–76.

102. Vertes, R. P., Kinney, G. G., Kocsis, B. and Fortin, W. J., Pharmacological suppression of the median raphe nucleus with serotonin(1A) agonists, 8-OH-DPAT and buspirone, produces hippocampal theta rhythm in the rat. *Neuroscience*, 1994, **60**, 441–451.

103. Vinogradova, O. S., Expression, control, and probable functional significance of the neuronal theta rhythm. *Progress in Neurobiology*, 1995, **45**, 523–583.

104. Whishaw, I. Q. and Vanderwolf, C. H., Hippocampal EEG and behavior: effects of variation in body temperature and relation of EEG to vibrissae movement, swimming and shivering. *Physiology and Behavior*, 1971, **6**, 391–397.

105. Winson, J., Patterns of hippocampal theta rhythm in the freely moving rat. *Electroencephalography and Clinical Neurophysiology*, 1974, **36**, 291–301.

106. Winson, J., Hippocampal theta rhythm. I. Depth profiles in the curarized rat. *Brain Research*, 1976, **103**, 57–70.

107. Winson, J., Behaviorally dependent neuronal gating in the hippocampus. In The Hippocampus, Vol. 4, ed. R. L. Isaacson and K. H. Pribram. Plenum Press, New York, 1986, pp. 77–91.

108. Winson, J. and Abzug, Z., Neuronal transmission through hippocampal pathways dependent upon behavior. *Journal of Neurophysiology*, 1978, **41**, 716–732.

109. Wu, K. and Leung, L. S., Functional connections between CA3 and the dentate gyrus and CA1 revealed by field potential analysis. *Hippocampus*, Submitted.

110. Ylinen, A., Soltesz, I., Bragin, A., Penttonen, M., Sik, A. and Buzsaki, G., Intracellular correlates of hippocampal theta rhythm in identified pyramidal cells, granule cells, and basket cells. *Hippocampus*, 1995, **5**, 78–90.

111. Yu, H. W. and Leung, L. S., Oscillatory driving of hippocampal CA1 cells in vitro. *Neuroscience Abstracts*, 1993, **19**, 356.

112. Zhao, D. and Leung, L. S., Effects of hippocampal kindling on paired-pulse response in CA1 in vitro. *Brain Research*, 1991, **564**, 220–229.

113. Zucker, R. S., Short-term synaptic plasticity. *Annual Review of Neuroscience*, 1989, **12**, 13–31.